HHS Public Access

Author manuscript

Biochem Biophys Res Commun. Author manuscript; available in PMC 2014 April 19.

Published in final edited form as:

Biochem Biophys Res Commun. 2013 April 19; 433(4): 396–400. doi:10.1016/j.bbrc.2013.02.082.

Functional inhibition of UQCRB suppresses angiogenesis in zebrafish

Yoon Sun Cho[a], **Hye Jin Jung**[a], **Seung Hyeok Seok**[b], **Alexander Y. Payumo**[c], **James K. Chen**[c], and **Ho Jeong Kwon**[a,*]

[a]Chemical Genomics National Research Laboratory, Department of Biotechnology, Translational Research Center for Protein Function Control, College of Life Science & Biotechnology, Yonsei University, Seoul 120-749, Republic of Korea

[b]Department of Microbiology and Immunology, Institute for Experimental Animals, Seoul National University College of Medicine, Seoul 110-799, Republic of Korea

[c]Department of Chemical and Systems Biology, Stanford University School of Medicine, Stanford, CA 94305, USA

Abstract

As a subunit of mitochondrial complex III, UQCRB plays an important role in complex III stability, electron transport, and cellular oxygen sensing. Herein, we report UQCRB function regarding angiogenesis *in vivo* with the zebrafish (*Danio rerio*). UQCRB knockdown inhibited angiogenesis in zebrafish leading to the suppression of VEGF expression. Moreover, the UQCRB-targeting small molecule terpestacin also inhibited angiogenesis and VEGF levels in zebrafish, supporting the role of UQCRB in angiogenesis. Collectively, UQCRB loss of function by either genetic and pharmacological means inhibited angiogenesis, indicating that UQCRB plays a key role in this process and can be a prognostic marker of angiogenesis- and mitochondria-related diseases.

Keywords

Angiogenesis; Mitochondria; UQCRB; Zebrafish

1. Introduction

The mitochondrion is primary energy source of the cell, bearing five oxidative phosphorylation complexes that regulate in ATP synthesis [1]. Of the five complexes, complex III is responsible for electron transport, ubisemiquione radical stabilization, and cellular oxygen sensing [2]. Notably, complex III deficiency is associated with lactic acidosis, hypoglycemia, encelopathy and other human disorders [3]. Recent reports provide evidence that deletion of the gene encoding UQCRB (ubiquinol-cytochrome c reductase binding protein), a complex III subunit, causes a defect in complex III function, resulting in

*Corresponding author. Fax: +82 2 362 7265. kwonhj@yonsei.ac.kr (H.J. Kwon).

hypoglycemia and lactic acidosis [4]. Furthermore, two SNPs of UQCRB were found in colorectal cancer, implying its potential as a prognostic marker for cancer [5]. Also, UQCRB is overexpressed in liver cancer cells, and copy number variation was found in cervical cancer and may be used as a cellular marker for cervical cancer diagnosis [6]. Jung et al. demonstrated that UQCRB plays a key role in VEGF signaling and regulates angiogenesis, and that terpestacin is the small molecule that binds to UQCRB [7]. Given these interesting roles, the present paper focuses on mitochondria complex III subunit UQCRB, and its possible role in angiogenesis *in vivo*.

The zebrafish is an ideal animal model for studying vascular development because of its tissue transparency and short development time [8,9]. In addition, gene function is readily interrogated in this system using morpholino antisense oligonucleotides or pharmacological agents [10–13]. Indeed, Tg(*fli1a:EGFP*)^{y1} transgenic zebrafish is widely used to visualize vasculogenesis and angiogenesis [14,15]. Vasculogenesis is the formation of new blood vessels, including those in the dorsal aorta and the posterior cardinal vein of the tail [16]. Vasculogenesis is followed by angiogenesis, which is the sprouting and extension of the intersegmental vessels (ISVs) from the dorsal aorta. Complete ISVs form the T-branch at the most dorsal side of the trunk, known as the dorsal longitudinal anastomotic vessel (DLAV). By evaluating the formation of complete ISVs in developing zebrafish, angiogenesis inhibition can be easily assessed for small-molecule or morpholino effects.

Herein, we report *in vivo* functional studies of UQCRB in respect with angiogenesis using the zebrafish system. Tg(*fli1a:EGFP*)^{y1} zebrafish embryos were used to visualize and analyze angiogenesis inhibition by downregulation of UQCRB function. UQCRB activity was reduced by knockdown with a *uqcrb*-MO or a UQCRB-targeting small molecule, terpestacin, treatment, leading to the inhibition of blood vessel growth. This is the first functional characterization of UQCRB *in vivo*, providing evidence that UQCRB plays an important role in angiogenesis.

2. Materials and methods

2.1. Zebrafish husbandry

Zebrafish were maintained on 14 h light/dark cycle at 28 °C. All experiments involving zebrafish were performed according to the National Institute of Health guidelines. Embryos were collected and raised in E3 media or ringer's solution according to standard protocol [17].

2.2. Morpholino injection and small molecule treatment

Zebrafish were injected in E3 media or ringer's solution at the one-cell stage with 1 or 2 ng/embryo morpholino oligonucleotides (MO). MO was obtained from Gene Tools (Philomath, OR) with the following sequence to block 5′ translation of UQCRB: 5′-GTGCCCTCGCCGCCATTTTTGTTCT-3′. DMSO and terpestacin stock solution (10 mg/mL in DMSO) were dissolved in ringer's solution to appropriate concentrations. Final volume of compounds did not exceed 1% of the total volume. Embryos were added to the solutions at one cell stage.

2.3. Microscopy imaging

Tricaine supplied in E3 media or ringer's solution (0.6%, w/v) was used to anesthetize the embryos for imaging. Anesthesized embryos were immobilized in 0.5% (w/v) low melting pointing agarose (Sigma–Aldrich, Saint Louis, MO) on slide glass. Microscopy images of zebrafish were taken with Leica S6E.

2.4. RNA isolation, RT-PCR analysis and primer construction

Zebrafish total RNA was isolated with RNeasy Mini kit (Qiagen) according to the manufacturer's protocol or with Trizol (Invitrogen, Carlsbad, CA) followed by precipitation with isopropanol, washing with 70% ethanol, and elution with DEPC treated water. Total RNA (5 μg) was reversibly transcribed by Molony murine leukemia virus reverse transcriptase (Invitrogen, Carlsbad, CA) using Oligo-d(T)15 primer in a final volume of 40 μL. cDNA mixture (2 μL) was used for PCR amplification of the specific gene with exTaq (Takara Bio Inc, Japan). SuperScript III One-Step RT-PCR System with Platinum Taq DNA Polymerase kit (Invitrogen, Carlsbad, CA) was applied according to the manufacturer's protocol for terpestacin treated embryos. Primers used for *vegfa* and *β-actin* are as follows: *vegfa* forward: CAGCTGTCAAGAGTGCCTACATAC, *vegfa* reverse: CATCAGGGTACTCCTGCTGAATTTC, *β-actin* forward: CGAGCTGTCTTCCCATCCA, *β-actin* reverse: TCACCAACGTAGCTGTCTTTCTG.

2.5. Statistical analysis

All statistical analyses were calculated with Graphpad Prism (ver. 5.00 for Windows, Graph Pad Software, San Diego, CA USA, www.graphpad.com). Results are expressed as mean ± standard error (± SEM). Student's *t*-tests were used to determine statistical significance between control and test groups. ANOVA (Turkey test) was used to determine statistical significance between three test groups. A *p*-valueless than 0.05 was considered statistically significant (* indicates $p < 0.05$, ** indicates $p < 0.001$, *** indicates $p < 0.0001$).

3. Results

3.1. Zebrafish angiogenesis is inhibited by UQCRB knockdown

To investigate the biological function of UQCRB in zebrafish, the translation blocker morpholino specific to *uqcrb* (*uqcrb*-MO) was applied. *Uqcrb*-MO was injected into Tg(*fli1a:EGFP*)^{y1} embryos at the one-cell stage to knockdown UQCRB. ISVs were detected at 30 h post fertilization (hpf). *Uqcrb*-MO dose dependently inhibited angiogenesis at 30 hpf starting from 1 ng. Two nanograms of *uqcrb*-MO completely inhibited angiogenic sprouting but vasculogenesis was not affected (Fig. 1A). The percentage of angiogenesis-inhibited embryos was 55.3% at 1 ng, which increased up to 78.0% at 2 ng (Fig. 1B). Angiogenic sprouts and ISVs were examined in UQCRB knockdown embryos starting from 24 to 36 hpf, the timeframe for angiogenesis in wildtype zebrafish. Normal dorsal aorta was detected in all embryos at all timeframes. At 24 hpf, the average number of angiogenic sprouts were 22 for control, 5.7 for *uqcrb*-MO 1 ng injected embryos and 1.8 for *uqcrb*-MO 2 ng injected embryos (Fig. 2A). Complete ISVs were not detected at 24 hpf in all embryos. At 30 hpf, an average of 19.5 complete ISVs that extended to form the DLAV were assessed in control embryos, but none in *uqcrb* morphants. The number of angiogenic sprouts decreased in a

dose-dependent manner compared to control; an average of 15 and 4.8 sprouts were examined in 1 ng and 2 ng *uqcrb*-MO injected embryos respectively. At 36 hpf, the average number of angiogenic sprouts increased to 28.5, 22.7, and 16.3 in control, 1 ng and 2 ng *uqcrb*-MO injected embryos, respectively. However, only three complete ISVs were formed in *uqcrb*-MO injected groups, compared to 25 for control embryos. The lengths of angiogenic sprouts were measured at each time frame (Fig. 2B). The average length of angiogenic sprouts decreased dose-dependently at all time frames in *uqcrb* morphants. Taken together, UQCRB knockdown with *uqcrb*-MO inhibits angiogenesis in zebrafish, in accordance to previous report with human cell lines tested for angiogenesis *in vitro* [7].

3.2. Zebrafish uqcrb morphants exhibit defects in morphology

Notably, the morphology of *uqcrb*-MO injected embryos showed ventral body curvature (Fig. 3A) in 55% of the 1 ng injected embryos and 73.4% of 2 ng injected embryos, which correlates with angiogenesis inhibition (Fig. 3B). Even with this developmental defect, the overall survival rate decreased only 21.3%, from 90% in control to 68.7% in *uqcrb*-MO 2 ng injected embryos (Fig. 3C).

3.3. Zebrafish angiogenesis is inhibited by the UQCRB-targeting small molecule terpestacin

Terpestacin is a natural product that inhibits angiogenesis by binding to UQCRB, which was reported by Jung et al. [7]. To test the possibility that terpestacin could also inhibit angiogenesis in zebrafish, we first compared the amino acid sequence of zebrafish UQCRB was compared with that of human UQCRB. UQCRB is highly conserved in human and zebrafish, with 72.1% amino acid sequence similarity (Fig. 4A). To investigate the effects of terpestacin on zebrafish angiogenesis, Tg(*fli1a:EGFP*)^{y1} embryos were cultured in the presence of the compound. Terpestacin treatment (20 μM) inhibited angiogenesis at 30 hpf, but the development of dorsal aorta was not affected and overall morphology was normal (Fig. 4B). Notably, terpestacin treated embryos exhibited high survival rate of 80.2% (Fig. 4C). The average number of complete ISVs was only 0.5 with terpestacin treatment compared to 19.5 in control embryos (Fig. 4D). The number of angiogenic sprouts significantly decreased from an average of 23.5 sprouts in control embryos to 15.3 in terpestacin-treated embryos (Fig. 4D). The average length of angiogenic sprouts decreased 54% in terpestacin-treated embryos compared to control (Fig. 4E). Overall, these results demonstrate that terpestacin inhibits angiogenesis in zebrafish.

3.4. Vegfa expression is reduced in terpestacin-treated zebrafish or uqcrb morphants

Of many angiogenic factors in angiogenesis signaling, VEGF is one of the important cytokine factors involved in UQCRB down-stream signaling. Therefore, *vegfa* expression levels were examined in both UQCRB knocked-down and terpestacin-treated embryos. UQCRB knockdown with 2 ng of *uqcrb*-MO resulted in decrease of overall *vegfa* expression level down to 56% compared to control (Fig. 4F). Likewise, embryos treated with terpestacin for 30 hpf resulted in significant decrease of *vegfa* level compared to control (Fig. 4F). Taken together, these results reveal that UQCRB mechanism includes VEGF transcription *in vivo*.

4. Discussion

Mitochondria complex III consists of 11 subunits including UQCRB, which acts in cooperation with angiogenic pathways. Loss of UQCRB function reduces angiogenic signaling *in vitro*, yet detailed functional characterization is needed to explain its role in biological systems. Therefore, we investigated the possible role of UQCRB in angiogenesis with the zebrafish system, resulting in a clearer understanding of UQCRB loss of function in relation to angiogenesis. Mitochondria complexes control the general level of oxidative phosphorylation, (OXPHOS), by affecting the mitochondrial electron transport chain. In the case of complex I inhibition by metform in, angiogenesis is decreased along with VEGF levels with metformin treatment [18–20]. However Phoenix et al. reported that metformin could also induce angiogenesis through AMPK activation in ERα negative MDA-MB-435 breast cancer model [21]. Furthermore, complex V inhibition with oligomycin is reported to inhibit HIF-1α, the upstream effector of VEGF [22]. Although there were no reports with direct angiogenesis inhibition by oligomycin, HIF-1α inhibition in hypoxic tumor cells provides evidence to possible angiogenesis inhibition. Likewise, mitochondria complexes could affect angiogenesis through OXPHOS regulation [23,24].

Antisense and pharmacological disruption of UQCRB function inhibited angiogenesis in zebrafish, but did not affect vasculogenesis. Angiogenesis recovered in both *uqcrb* morphants and terpestacin-treated embryos after 48 hpf, possibly due to the transient or incomplete penetrance of these perturbations. Alternatively, there may be distinct temporal requirements for UQCRB during angiogenesis or UQCRB may play a supportive but not essential role in the sprouting and extension of blood vessels *in vivo*. We note that *uqcrb* morphants and terpestacin-treated embryos exhibit some phenotypic differences; *uqcrb* morpholinos can induce ventral body curvature while terpestacin causes a more significant loss of *vegf* expression. These differences may be due to the fact that the *uqcrb* morpholino prevents UQCRB expression while terpestacin only inhibits the biological activity of this mitochondrial complex III subunit, functionally distinct perturbations that may have divergent phenotypic consequences. The antisense oligonucleotide and/or small-molecule treatments may also have unanticipated, non-overlapping off-target effects. Finally, UQCRB may promote angiogenesis through both VEGF-dependent and VEGF-independent mechanisms. Further studies will be necessary to resolve these questions.

To our best knowledge, this is the first report on the functional characterization of UQCRB *in vivo*. UQCRB is involved in diseases related to mitochondria complex III, and in the present study UQCRB involvement in angiogenesis was revealed. These results implicate that UQCRB could be used in etiologic studies, especially regarding angiogenesis-related diseases. Furthermore, UQCRB could be used as a marker for angiogenesis, and drugs that specifically target UQCRB could be developed to introduce new therapeutic treatments. UQCRB transgenic studies would also provide in-depth evidence for its diverse potential in disease and facilitate mechanistic studies of mitochondria and UQCRB.

Acknowledgments

This study was partly supported by Grants from the National Research Foundation (NRF) of Korea, the Korean Government (MEST; 2009-0092964, 2010-0017984, 2012M3A9D1054 520), the Translational Research Center for

Protein Function Control and the National Junior Research Fellowship, NRF (2009-0083522, 2011-006165), the Center for Food and Drug Materials of Agriculture Science & Technology Development (PJ0079772012), the Rural Development Administration, and the Brain Korea 21 Project, and the National Institutes of Health (DP1 HD075622 to J.K.C.).

References

1. DiMauro S, Schon EA. Mitochondrial respiratory-chain diseases. N Engl J Med. 2003; 348:2656–2668. [PubMed: 12826641]
2. Crivellone MD, Wu MA, Tzagoloff A. Assembly of the mitochondrial membrane system. Analysis of structural mutants of the yeast coenzyme QH2-cytochrome C reductase complex. J Biol Chem. 1988; 263:14323–14333. [PubMed: 2844766]
3. de Lonlay P, Valnot I, Barrientos A, Gorbatyuk M, Tzagoloff A, Taanman JW, Benayoun E, Chretien D, Kadhom N, Lombes A, de Baulny HO, Niaudet P, Munnich A, Rustin P, Rotig A. A mutant mitochondrial respiratory chain assembly protein causes complex III deficiency in patients with tubulopathy, encephalopathy and liver failure. Nat Genet. 2001; 29:57–60. [PubMed: 11528392]
4. Haut S, Brivet M, Touati G, Rustin P, Lebon S, Garcia-Cazorla A, Saudubray JM, Boutron A, Legrand A, Slama A. A deletion in the human QP-C gene causes a complex III deficiency resulting in hypoglycemia and lactic acidosis. Hum Genet. 2003; 113:118–122. [PubMed: 12709789]
5. Lascorz J, Bevier M, Schonfels WV, Kalthoff H, Aselmann H, Beckmann J, Egberts J, Buch S, Becker T, Schreiber S, Hampe J, Hemminki K, Forsti A, Schafmayer C. Polymorphisms in the mitochondrial oxidative phosphorylation chain genes as prognostic markers for colorectal cancer. BMC Med Genet. 2012; 13:31. [PubMed: 22545919]
6. Wrzeszczynski KO, Varadan V, Byrnes J, Lum E, Kamalakaran S, Levine DA, Dimitrova N, Zhang MQ, Lucito R. Identification of tumor suppressors and oncogenes from genomic and epigenetic features in ovarian cancer. PLoS One. 2011; 6:e28503. [PubMed: 22174824]
7. Jung HJ, Shim JS, Lee J, Song YM, Park KC, Choi SH, Kim ND, Yoon JH, Mungai PT, Schumacker PT, Kwon HJ. Terpestacin inhibits tumor angiogenesis by targeting UQCRB of mitochondrial complex III and suppressing hypoxia-induced reactive oxygen species production and cellular oxygen sensing. J Biol Chem. 2010; 285:11584–11595. [PubMed: 20145250]
8. Lawson ND, Weinstein BM. Arteries and veins: making a difference with zebrafish. Nat Rev Genet. 2002; 3:674–682. [PubMed: 12209142]
9. Cross LM, Cook MA, Lin S, Chen JN, Rubinstein AL. Rapid analysis of angiogenesis drugs in a live fluorescent zebrafish assay, Arterioscler. Thromb Vasc Biol. 2003; 23:911–912.
10. Nasevicius A, Ekker SC. Effective targeted gene ‘knockdown’ in zebrafish. Nat Genet. 2000; 26:216–220. [PubMed: 11017081]
11. Summerton J, Weller D. Morpholino antisense oligomers: design, preparation, and properties. Antisense Nucleic Acid Drug Dev. 1997; 7:187–195. [PubMed: 9212909]
12. Tran TC, Sneed B, Haider J, Blavo D, White A, Aiyejorun T, Baranowski TC, Rubinstein AL, Doan TN, Dingledine R, Sandberg EM. Automated, quantitative screening assay for antiangiogenic compounds using transgenic zebrafish. Cancer Res. 2007; 67:11386–11392. [PubMed: 18056466]
13. Crawford AD, Liekens S, Kamuhabwa AR, Maes J, Munck S, Busson R, Rozenski J, Esguerra CV, de Witte PA. Zebrafish bioassay-guided natural product discovery: isolation of angiogenesis inhibitors from East African medicinal plants. PLoS One. 2011; 6:e14694. [PubMed: 21379387]
14. Lawson ND, Weinstein BM. In vivo imaging of embryonic vascular development using transgenic zebrafish. Dev Biol. 2002; 248:307–318. [PubMed: 12167406]
15. Wiens KM, Lee HL, Shimada H, Metcalf AE, Chao MY, Lien CL. Platelet-derived growth factor receptor beta is critical for zebrafish intersegmental vessel formation. PLoS One. 2010; 5:e11324. [PubMed: 20593033]
16. Childs S, Chen JN, Garrity DM, Fishman MC. Patterning of angiogenesis in the zebrafish embryo. Development. 2002; 129:973–982. [PubMed: 11861480]
17. Westerfield, M. The Zebrafish Book: a Guide for the Laboratory Use of Zebrafish (*Danio rerio*). third. Eugene, OR: University of Oregon Press; 1995.

18. Soraya H, Esfahanian N, Shakiba Y, Ghazi-Khansari M, Nikbin B, Hafezzadeh H, Dizaji NM, Garjani A. Anti-angiogenic effects of metformin, an AMPK activator, on human umbilical vein endothelial cells and on granulation tissue in rat. Iran J Basic Med Sci. 2012; 15:1202–1209. [PubMed: 23653852]
19. Tan BK, Adya R, Chen J, Farhatullah S, Heutling D, Mitchell D, Lehnert H, Randeva HS. Metformin decreases angiogenesis via NF-κB and Erk1/2/Erk5 pathways by increasing the antiangiogenic thrombospondin-1. Cardiovasc Res. 2009; 83:566–574. [PubMed: 19414528]
20. Ersoy C, Kiyici S, Budak F, Oral B, Guclu M, Duran C, Selimoglu H, Erturk E, Tuncel E, Imamoglu S. The effect of metformin treatment on VEGF and PAI-1 levels in obese type 2 diabetic patients. Diabetes Res Clin Pract. 2008; 81:56–60. [PubMed: 18358555]
21. Phoenix KN, Vumbaca F, Claffey KP. Therapeutic metformin/AMPK activation promotes the angiogenic phenotype in the ERα negative MDA-MB-435 breast cancer model. Breast Cancer Res Treat. 2009; 113:101–111. [PubMed: 18256928]
22. Gong Y, Agani FH. Oligomycin inhibits HIF-1α expression in hypoxic tumor cells. Am J Physiol Cell Physiol. 2005; 288:C1023–C1029. [PubMed: 15840558]
23. Richard DE, Berra E, Pouyssegur J. Angiogenesis: how a tumor adapts to hypoxia. Biochem Biophys Res Commun. 1999; 266:718–722. [PubMed: 10603309]
24. Pathania D, Millard M, Neamati N. Opportunities in discovery and delivery of anticancer drugs targeting mitochondria and cancer cell metabolism. Adv Drug Deliv Rev. 2009; 61:1250–1275. [PubMed: 19716393]

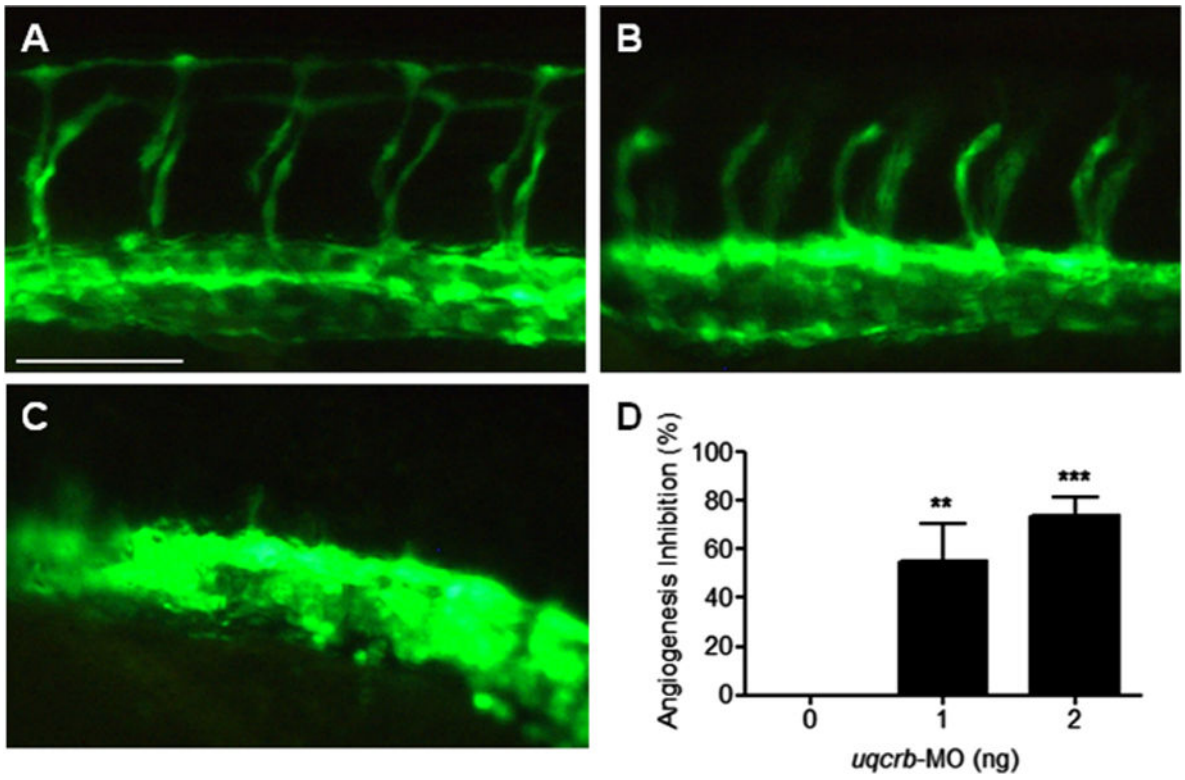

Fig. 1.

Knockdown of UQCRB inhibits zebrafish angiogenesis. (A) Complete ISVs at 30 hpf in control embryos. (B) Inhibition of angiogenesis in 1 ng *uqcrb*-MO injected embryos ($n = 30$, representative image from three independent trials). (C) Inhibition of angiogenesis in 2 ng *uqcrb*-MO injected embryos ($n = 30$, representative image from three independent trials). (D) Dose-dependent inhibition of angiogenesis in *uqcrb*-MO injected embryos. Quantified data are presented as mean ± SEM compared to control (**indicates $p < 0.001$, ***indicates $p < 0.0001$). Scale bar indicates 100 μm.

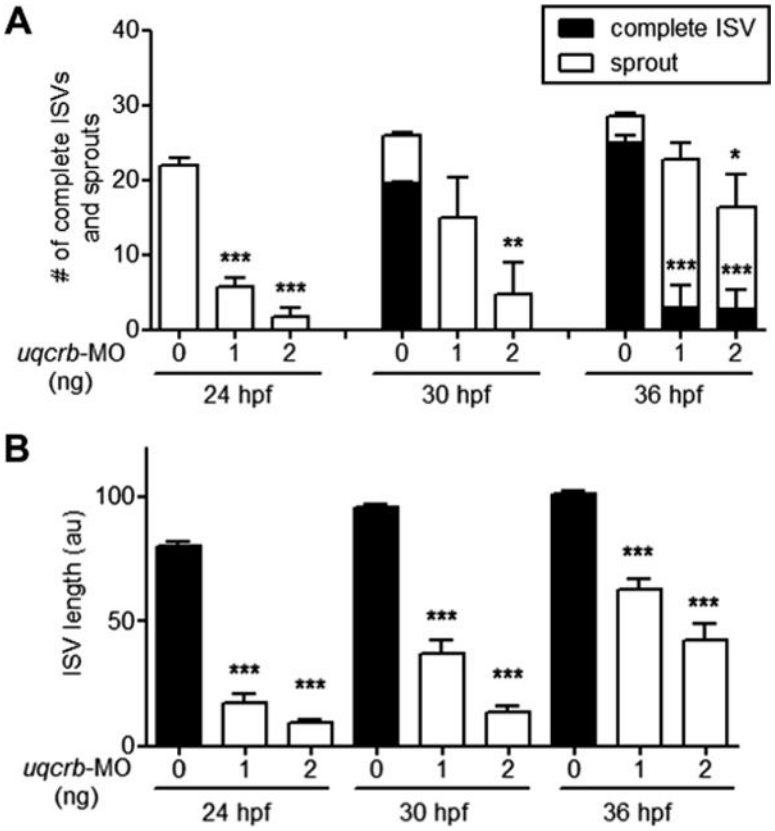

Fig. 2.

(A) Angiogenic sprouts were detected starting from 24 hpf in control embryos. An average of 19.5 complete ISVs was detected in control embryos starting from 30 hpf. Complete ISVs were not detected in 1 and 2 ng *uqcrb*-MO injected embryos until 36 hpf. Only an average of three complete ISVs was examined in *uqcrb*-MO injected embryos (n = 5). (B) Angiogenic sprout length showed a great difference between control and dose-dependently decreased in *uqcrb*-MO injected embryos at all time frames. All quantified data are presented as mean ± SEM (*indicates $p < 0.05$, **indicates $p < 0.001$, ***indicates $p < 0.0001$).

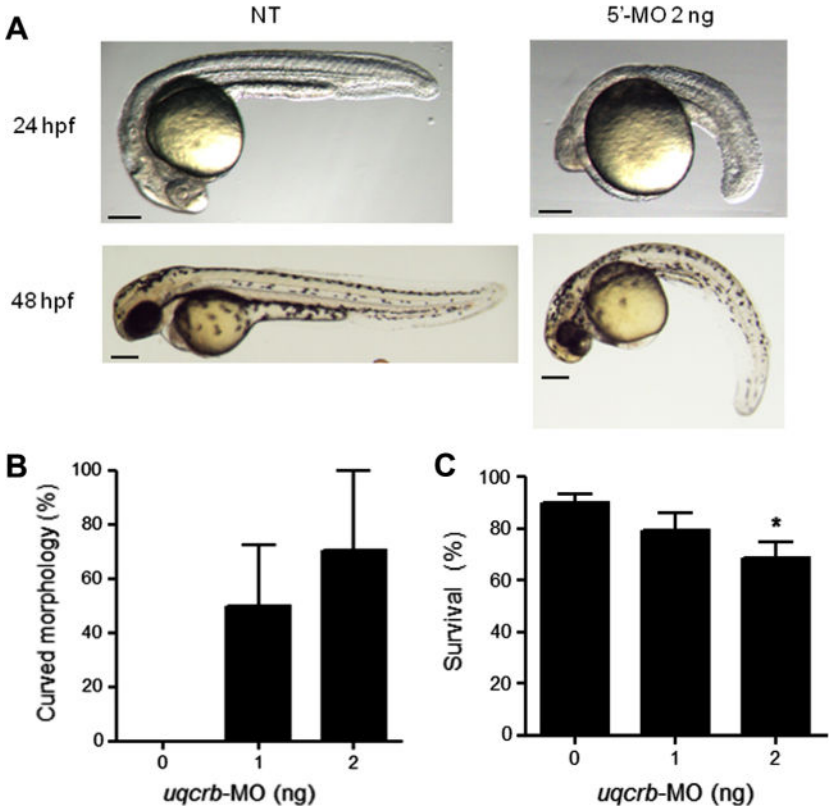

Fig. 3.

(A) Body curvature morphology was detected in 2 ng *uqcrb*-MO injected embryos at 24 and 48 hpf (n = 30, three independent trials). (B) Number of curved embryos increased dose-dependently in *uqcrb*-MO injected groups. (C) Survival rates decreased only down to 68.7% in 2 ng *uqcrb*-MO injected embryos. All quantified data are presented as mean ± SEM (*indicates $p < 0.05$). Scale bars indicate 200 μm.

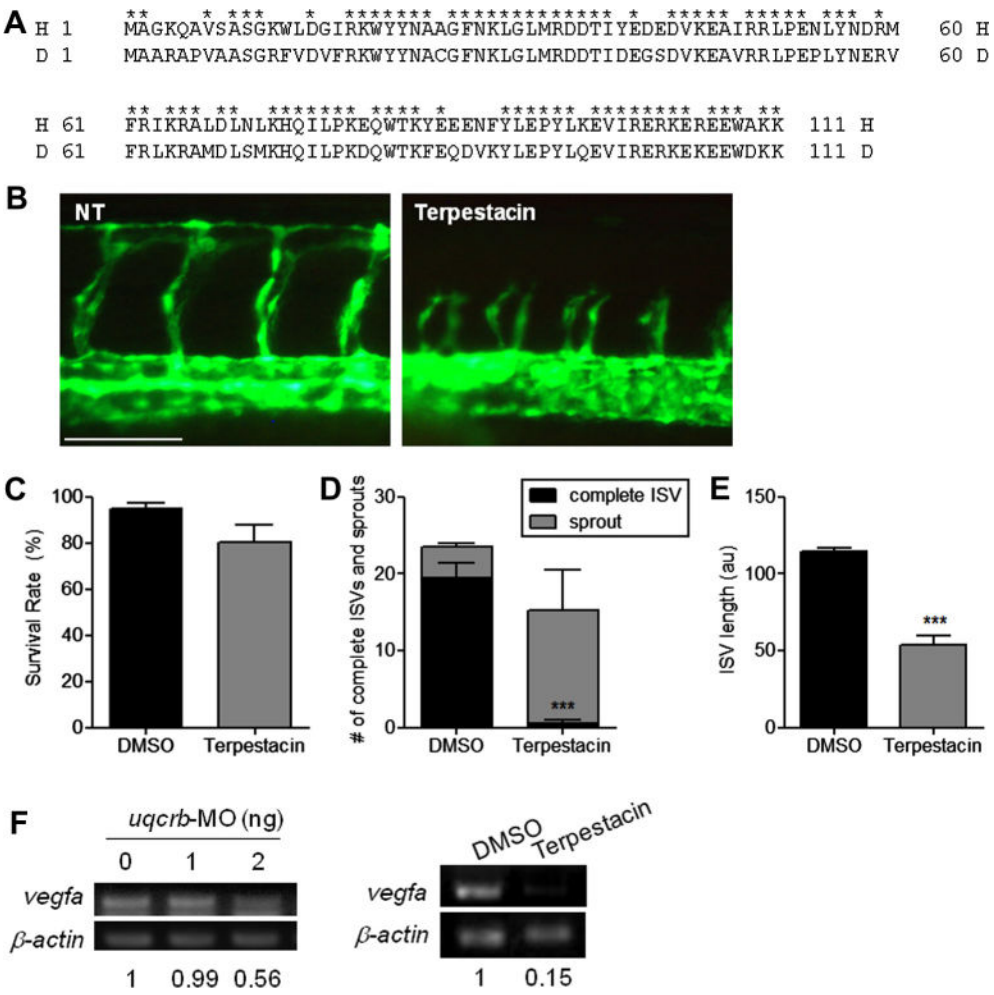

Fig. 4.

(A) UQCRB is conserved in human and zebrafish. The amino acid sequence alignment shows 72% similarity between human and zebrafish. (H: *Homo sapiens*, D: *Danio rerio*) Asterisks represent the identical amino acid of two sequences. (B) Terpestacin inhibited angiogenesis in zebrafish at 30 hpf. (C) The survival rate for terpestacin treated embryos decreased mildly to 80%. (D) Only an average of 0.5 complete ISV was examined in terpestacin treated embryos. The average number of angiogenic sprouts decreased to 15.2, compared to control embryos which had an average of 23 sprouts. (E) The length of angiogenic sprouts in terpestacin treated embryos decreased 47% compared to control. All quantified data are presented as mean ± SEM (***indicates $p < 0.0001$). (F) *Vegfa* levels decreased in *uqcrb*-MO injected embryos and terpestacin treated embryos at 30 hpf. Numbers indicate *vegfa* expression ratio compared to control (n = 35, three independent trials). Scale bar indicates 100 μm.